Molecular Orbital Description of the Bonding and Reactivity of the Platinum η^3-Propargyl Complex $[(\eta^3\text{-}CH_2CCPh)Pt(PPh_3)_2]^+$

John P. Graham, Andrew Wojcicki,* and Bruce E. Bursten*

Department of Chemistry, The Ohio State University, Columbus, Ohio 43210

Received September 30, 1998

The recently prepared η^3-propargyl complex $[(\eta^3\text{-}CH_2CCPh)Pt(PPh_3)_2]^+$ (**1**) exhibits unusual regioselectivity in reactions involving nucleophilic addition to the propargyl ligand. Fenske−Hall approximate molecular orbital calculations and density functional calculations have been carried out to study the structure, bonding, and reactivity of **1**. The calculations suggest that the principal bonding interaction between Pt and the propargyl ligand occurs through the terminal carbon atoms of the ligand, despite the observed short Pt−central carbon distance. Optimized geometries for model complexes calculated by density functional methods agree well with the reported crystal structure of **1**. The observed nucleophilic addition to the central carbon of the propargyl ligand is suggested to occur through a charge-controlled mechanism, assisted by the presentation of a low-lying acceptor orbital on the central carbon along the reaction path.

Introduction

Transition-metal η^1-propargyl and η^1-allenyl complexes have been known since the 1960s.[1] The propargyl (A) and allenyl ligands (B) are isomeric. The η^1 com-

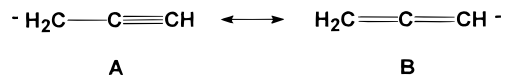

A B

plexes have been studied extensively due to their possible roles in catalytic reactions and their usefulness as starting materials in organic synthesis.[2] The unsaturated nature of the ligand provides a starting point for the synthesis of five-membered heterocyclic and homocyclic organic rings[3] and many binuclear and trinuclear organometallic complexes.[2]

Complexes containing η^3 bonding modes of propargyl/allenyl ligands were discovered only recently, including complexes of Mo, Re, Zr, Pt, and Pd.[4] This new class of organometallic π complexes has been the subject of much interest in recent years because of unusual structural properties and reactivity.[5] Our previous work in this area has included the Pt complex $[(\eta^3\text{-}CH_2CCPh)Pt(PPh_3)_2]^+$ (**1**), which has demonstrated an unusually high propensity to undergo addition of nucleophilic reagents.[4c] Nucleophiles such as PMe_3, Br^-, and CO add to the metal center, resulting in decreased hapticity of the propargyl/allenyl ligand and formation of η^1-allenyl and η^1-propargyl complexes. The products formed during these reactions are highly dependent on the incoming nucleophile. For example, addition of Br^- results in the formation of square-planar η^1-propargyl complexes only, largely the trans isomer, whereas the addition of PMe_3 results in the formation of an η^1-allenyl complex only.

Reactions involving nucleophilic addition to the η^3-propargyl ligand will be the primary focus of this paper. The nucleophile adds to the central carbon atom of the propargyl ligand, in contrast to η^3-allyl complexes, where nucleophilic addition is mostly observed to a terminal C atom. Well-known exceptions to this rule are the complexes $Cp_2M(C_3H_5)^+$ (M = Mo, W).[6] Extended Hückel MO calculations have been used to explain the unusual regioselectivity of nucleophilic addition in these complexes.[7,8] More recently, nucleophilic addition to the central carbon of (η^3-allyl)palladium complexes by some more stabilized carbon nucleophiles has been reported.[9] However, the predominantly observed sites of addition are the terminal carbon atoms of the allyl ligand. Addition to the propargyl ligand is observed for nucleophiles of the general form NuH: i.e., those with a transferable proton. The resultant products are η^3-allyl

(1) Wojcicki, A. *Ann. N. Y. Acad. Sci.* **1974**, *239*, 100.
(2) For a review of η^1-propargyl/allenyl chemistry, see: Wojcicki, A.; Shuchart, C. E. *Coord. Chem. Rev.* **1990**, *105*, 35.
(3) (a) Rosenblum, M. *Acc. Chem. Res.* **1974**, *7*, 122. (b) Wojcicki, A. In *Fundamental Research in Organometallic Chemistry*; Tsutsui, M., Ishii, Y., Huang, Y., Eds.; Van Nostrand-Reinhold: New York, 1982; pp 569−597. (c) Welker, M. E. *Chem. Rev.* **1992**, *92*, 97.
(4) (a) Mo: Krivykh, V. V.; Taits, E. S.; Petrovskii, P. V.; Struchkov, Y. T.; Yanovski, A. I. *Mendeleev Commun.* **1991**, 103. (b) Zr: Blosser, P. W.; Gallucci, J. C.; Wojcicki, A. *J. Am. Chem. Soc.* **1993**, *115*, 2994. (c) Pt: Blosser, P. W.; Schimpff, D. G.; Gallucci, J. C.; Wojcicki, A. *Organometallics* **1993**, *12*, 1993. (d) Re: Casey, C. P.; Yi, C. S. *Organometallics* **1990**, *9*, 2413. (e) Pd: Baize, M. W.; Blosser, P. W.; Plantevin, V.; Schimpff, D. G.; Gallucci, J. C.; Wojcicki, A. *Organometallics* **1996**, *1*, 15. (f) Pt: Huang, M. T.; Chen, J. T.; Lee, G. H.; Wang, Y. *J. Am. Chem. Soc.* **1993**, *115*, 1170. (g) Pt: Stang, P. J.; Crittell, C. M.; Arif, A. M. *Organometallics* **1993**, *12*, 4799. (h) Pd: Ogoshi, S,; Tsutsumi, K.; Kurosawa, H. *J. Organomet. Chem.* **1995**, *493*, C19.
(5) See, for example: (a) Wojcicki, A. *New J. Chem.* **1994**, *18*, 61. (b) Doherty, S.; Corrigan, G. F.; Carty, A. G.; Sappa, E. *Adv. Organomet. Chem.* **1995**, *37*, 39.
(6) Ephretikhine, M.; Francis, B. R.; Green, M. L. H.; Mackenzie, R. E.; Smith, M. J. *J. Chem. Soc., Dalton Trans.* **1977**, 1131.
(7) Lauher, J. W.; Hoffmann, R. *J. Am. Chem. Soc.* **1976**, *98*, 1729.
(8) Curtis, D. M.; Eisenstein, O. *Organometallics* **1984**, *3*, 887.
(9) (a) Castano, A. M.; Aranyos, A.; Szabo, K. J.; Bäckvall, J. E. *Angew. Chem., Int. Ed. Engl.* **1995**, *34*, 2551. (b) Aranyos, A.; Szabo, K. J.; Castano, A. M.; Bäckvall, J. E. *Organometallics* **1997**, *16*, 1058.

10.1021/om9808209 CCC: $18.00
Publication on Web 02/05/1999

complexes. The reaction of **1** with $Na[CH(CO_2Me)_2]$, which results in the formation of a zwitterionic η^3-allyl complex, illustrates the unusually high propensity for **1** to react in this manner.[4c] The structurally analogous Pd counterpart of complex **1** has also been prepared. It has been shown to undergo reactions similar to those of **1**, although somewhat less readily.[4e]

In this contribution, we will use Fenske−Hall and density functional electronic structure calculations to address the structure, bonding, and reactivity of model complexes of **1** and likely intermediates on its reactions with nucleophiles.

Computational Details

Fenske−Hall Calculations.[10] Fenske−Hall calculations were carried out on a Pentium-based personal computer. All atomic basis functions were generated by a least-squares fit of Slater-type orbitals to the atomic orbitals from Herman−Skillman atomic calculations.[11] Contracted double-ζ representations were used for the Pt 5d, C 2p, and P 3p atomic orbitals. An exponent of 1.16 was used for the hydrogen 1s AOs.[12] The basis functions for Pt were derived for the +2 oxidation state with fixed 6s and 6p exponents of 2.0. The basis functions for C and P were derived from the 0 oxidation state.

The CH_2CCPh^- ligand of **1** was modeled as CH_2CCH^-. The lowest lying occupied valence molecular orbital of this model ligand was deleted from the variational orbitals.[13] The H atom replacing the Ph group was placed along the Pt−Ph vector, 1.08 Å from the C atom. The PPh_3 ligand was modeled with PH_3, which had an H−P−H angle of 102°.[14] The model propargyl complex $[(\eta^3\text{-}CH_2CCH)Pt(PH_3)_2]^+$ (**1′**) was idealized to C_s symmetry. The structure of the model allyl complex $[(\eta^3\text{-}C_3H_5)Pt(PH_3)_2]^+$ (**2′**) was derived from the crystal structure of $[(\eta^3\text{-}C_3H_5)Pt(PCy_3)_2]^+$ (**2**)[15] and was also idealized to C_s symmetry. The structure of the hypothetical C_s metallacyclobutene complex $(\eta^2\text{-}CH_2CHCH)Pt(PH_3)_2$ (**3′**) was assumed to have standard C=C and C−C bond distances,[16] a C−C−C angle of 120°, and $Pt-C_{term}$ and Pt−P bond lengths equal to those in **1**. The numbering convention used to label the carbon atoms in complexes **1′**, **2′**, and **3′** is presented in Chart 1.

Density Functional Calculations. The Amsterdam density functional (ADF) program,[17] running on a Pentium-based computer, was used for all calculations. All geometry optimizations were carried out with inclusion of Becke's nonlocal exchange[18] and Perdew's nonlocal correlation[19] corrections (BP functional). A double-ζ basis set was chosen for C and H, and a triple-ζ basis was used for Pt. A double-ζ basis set with polarization functions was used for P. In nonrelativistic calculations, the frozen core approximation[20] was used to treat the 1s orbital of C, the 1s, 2s, and 2p orbitals of P, and the [Kr]4d core of Pt. For relativistic calculations, relativistic core potentials were computed using the ADF auxiliary program DIRAC. Scalar relativistic effects were accounted for in the calculations by use of the quasi-relativistic method[21] of ADF.

Chart 1

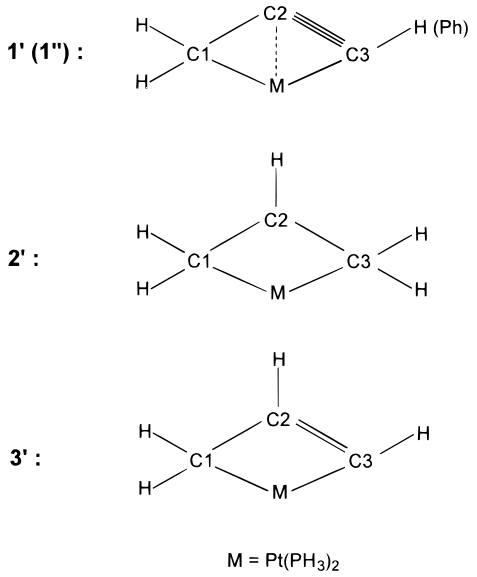

Results and Discussion

Structure of the Bound η^3-Propargyl/Allenyl Ligand. The crystallographic C1−C2 and C2−C3 bond distances observed in the $H_2C1C2C3Ph$ ligand in **1**, 1.39 and 1.23 Å, respectively, are intermediate between C−C single and double and C−C double and triple bonds, respectively.[4c] Thus, the bond lengths are consistent with resonance between propargyl and allenyl structures. From here on, the ligand will be referred to as an *η^3-propargyl* ligand for convenience.

Both of the resonance forms of the η^3-propargyl ligand would be expected to lead to a linear geometry at the central carbon atom. The $\eta^3\text{-}CH_2CCPh^-$ ligand in complex **1** has a C−C−C angle (θ) of 152°,[4c] which clearly is not linear but is also considerably larger than that observed in most η^3-allyl complexes (ca. 120°).[22] Thus, we will first address the changes in the electronic structure of the η^3-propargyl ligand as the C−C−C angle is reduced. We will then look closer at the metal−ligand interactions that induce the bending in the ligand.

A Walsh diagram showing the effect on the orbitals of varying the C−C−C angle of H_2CCCH^- from 180 to 100° is given in Figure 1. In the linear geometry, the anion is planar (C_{2v} symmetry) with one, two, and two pπ orbitals available on C1, C2, and C3, respectively. The $1b_1$, $2b_1$, and $3b_1$ MOs are the bonding, nonbonding, and antibonding combinations of the out-of-plane π orbitals; this π system extends over all three carbon atoms of the ligand. The $1b_2$ and $2b_2$ MOs are the bonding and antibonding in-plane π orbitals, which are localized between C2 and C3. The $1b_1$, $1b_2$, and $2b_1$ MOs are occupied, which leads to a localized π bond between C2 and C3 and a delocalized π bond among all three carbon atoms. This MO description is therefore consistent with the resonance structures shown above.

(10) Hall, M. B.; Fenske, R. F. *Inorg. Chem*. **1972**, *11*, 768.
(11) Bursten, B. E.; Jensen, J. R.; Fenske, R. F. *J. Chem. Phys.* **1978**, *68*, 3320.
(12) Hehre, W. J.; Stewart, R. F.; Pople, J. A. *J. Chem. Phys.* **1969**, *51*, 2657.
(13) Lichtenberger, D. L.; Fenske, R. F. *J. Chem. Phys.* **1969**, *51*, 4247.
(14) Clayton, T. Ph.D. Dissertation, The Ohio State University, Columbus, OH, 1988.
(15) Smith, J. D.; Oliver, J. D. *Inorg. Chem*. **1978**, *9*, 2585.
(16) Pople, J. A.; Gordon, M. *J. Am. Chem. Soc.* **1967**, *89*, 4253.
(17) (a) Amsterdam Density Functional Program, Versions 1.1, 2.0, and 2.1; Theoretical Chemistry, Vrije Universiteit, Amsterdam. (b) Baerends, E. J.; Ellis, D. E.; Ros, P. *Chem. Phys.* **1973**, *2*, 41. (c) te Velde, G.; Baerends, E. J. *J. Comput. Phys.* **1992**, *99*, 84.
(18) Becke, A. D. *Phys. Rev.* **1988**, *A38*, 2398.
(19) Perdew, J. P. *Phys. Rev*. **1986**, *B33*, 8822; **1986**, *B34*, 7406 (erratum).
(20) Baerends, E. J.; Ellis, D. E.; Ros, P. *Chem. Phys.* **1973**, *2*, 42.
(21) Ziegler, T.; Baerends, E. J.; Snijders, J. G.; Ravenek, W. *J. Phys. Chem*. **1989**, *93*, 3050.
(22) Clarke, H. L. *J. Organomet. Chem*. **1974**, *80*, 155.

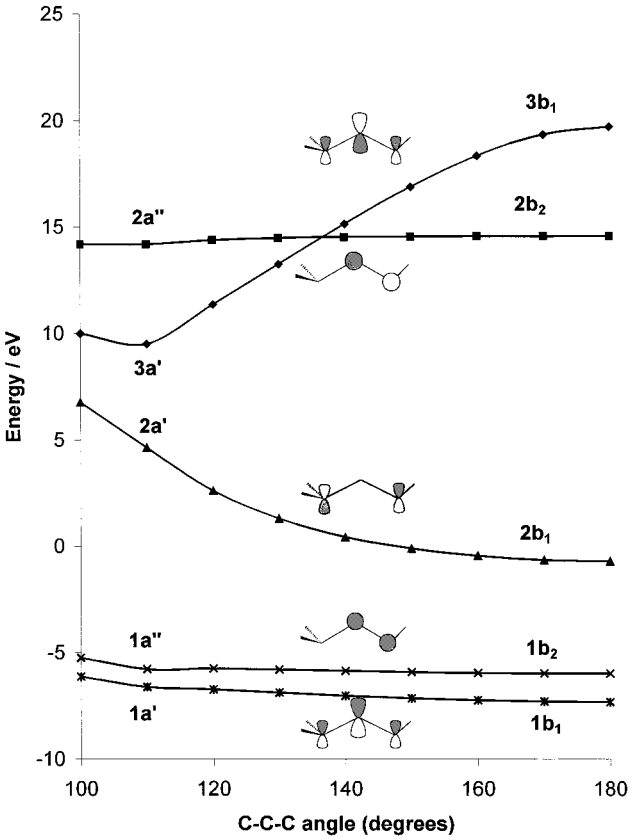

Figure 1. Walsh diagram for the propargyl ligand (H_2CCCH^-), as based on Fenske−Hall calculations. The MO labels are given under both C_{2v} and C_s symmetry.

Decreasing the C−C−C angle, with concomitant pyramidalization at C1 and trigonalization at C3, leads to some expected and unexpected effects. First, the $1b_2$ and $2b_2$ MOs are, as expected, largely unaffected by this geometric change. These MOs become the out-of-plane 1a″ and 2a″ MOs of the bent C_s ligand. The $1b_1$ MO, which becomes the 1a′ under C_s symmetry, rises only slightly upon bending; the decrease in C1−C2 and C2−C3 π bonding is largely offset by an increase in the direct bonding interactions between C1 and C3. The $2b_1$ (2a′) HOMO increases in energy on bending, as antibonding interactions between the terminal C atoms increase. This antibonding interaction becomes most significant at $\theta < 150°$. The $3b_1$ (3a′) MO shows the most dramatic change upon bending. This orbital drops considerably on going from 180 to 110°, which can be attributed to a decrease in the C1−C2 and C2−C3 antibonding interactions and an increase in the C1−C3 bonding interaction on bending. For the isolated anionic ligand, the 3a′ orbital falls below the 2a″ orbital at $\theta \approx 135°$, at which point it becomes the LUMO. Hence, decreasing θ from 180 to 100° results in destabilization of the ligand through increasing the HOMO energy and (at $\theta < 135°$) decreasing the LUMO energy. As we will see, however, these adverse effects of bending are offset by an increase in the spatial overlap of the ligand orbitals with the Pt-$(PH_3)_2^{2+}$ $2b_1$ LUMO orbital in model complex **1′**. The C−C−C angle of 152° observed in **1** thus represents a compromise between destabilizing effects within the ligand and stabilizing effects of the metal ligand interactions.

Electronic Structure of $[(\eta^3\text{-}CH_2CCH)Pt(PH_3)_2]^+$ (1′). The molecular orbital diagram of the model complex **1′** is presented in Figure 2. We have presented the results in a fragment approach, in which the orbitals of the CH_2CCH^- ligand interact with those of a $Pt(PH_3)_2^{2+}$ fragment. It is seen that the most significant interaction between the two fragments occurs between the 2a′ HOMO of the CH_2CCH^- ligand and the $2b_1$ LUMO of the $Pt(PH_3)_2^{2+}$ fragment, which is a Pt 5d−PH_3 antibonding combination that is directed toward the organic ligand. The strong interaction of these frontier orbitals forms the occupied bonding 3a′ and unoccupied antibonding 6a′ MOs of **1′**. Contour plots of these two MOs are given in Figure 3. The occupied 3a′ MO represents the formation of Pt−C σ bonds, by analogy to the bonding in other metallacyclic systems.[23]

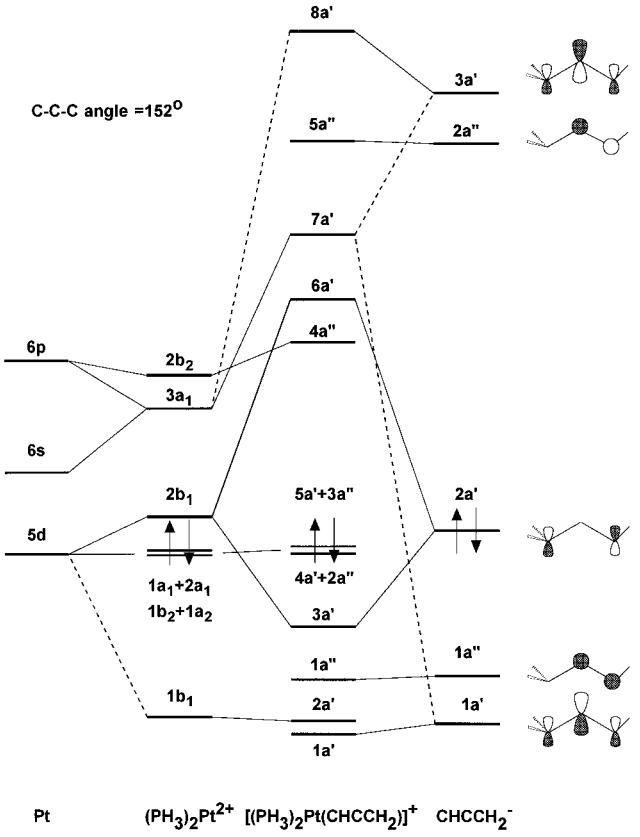

Figure 2. Molecular orbital diagram for the model propargyl complex **1′**, $[(PH_3)_2Pt(\eta^3\text{-}H_2CCCH)]^+$.

The 1a″ and 2a″ π orbitals of CH_2CCH^-, which are perpendicular to the Pt−C−C−C plane of **1′**, do not interact significantly with the metal fragment, mainly because of small overlap. Likewise, the 1a′ orbital of CH_2CCH^- interacts only weakly with the orbitals of $Pt(PH_3)_2^{2+}$; in addition to poor overlap, the low-lying 1a′ orbital is more energetically removed from the frontier orbitals of $Pt(PH_3)_2^{2+}$ than is the 2a′ MO of CH_2CCH^-. We are thus left with a rather simple description of the bonding between the two fragments as primarily involving one frontier orbital on each fragment, the 2a′ on CH_2CCH^- and $2b_1$ on the metal fragment. The LUMO of **1′** is largely composed of the Pt $6p_z$ AO, an observation that we will note in the next section in discussions of the reactivity of **1′**.

It is interesting to note that the 2a′ orbital of the CH_2CCH^- fragment has essentially no contribution

(23) Thorn, D. L.; Hoffmann, R. *Nouv. J. Chim.* **1979**, *3*, 39.

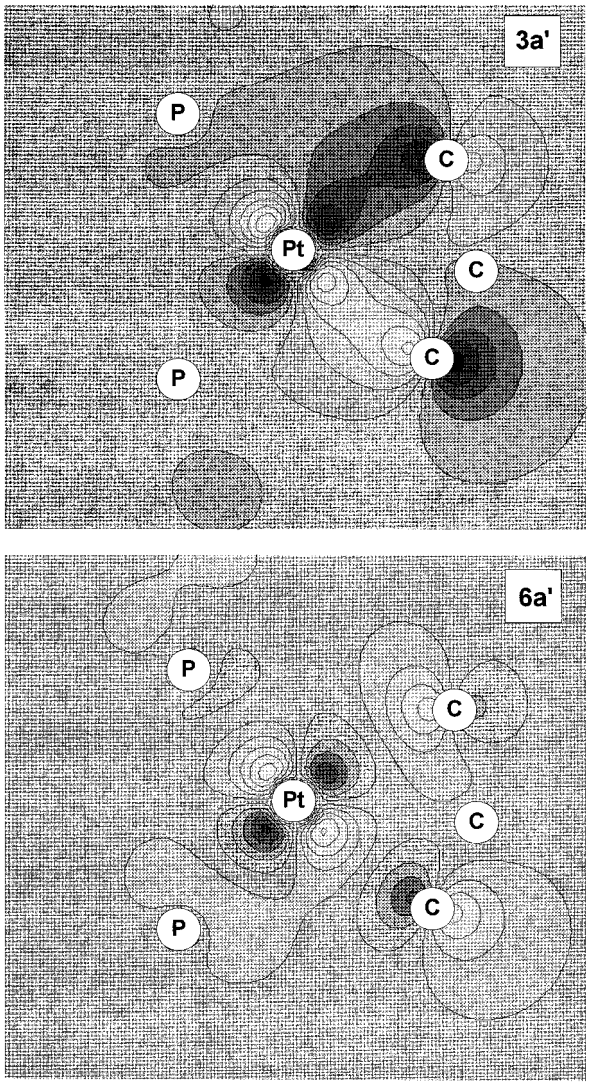

Figure 3. Contour plots of the 3a′ and 6a′ orbitals of complex **1′**.

Table 1. Fenske−Hall Mulliken Charges on the Carbon Atoms of Model Complexes 1′, 2′, and 3′[a]

	C1	C2	C3
propargyl complex (**1′**)	−0.18	+0.27	−0.24
allyl complex (**2′**)	−0.16	+0.17	−0.16
metallacyclobutene complex (**3′**)	−0.28	+0.23	−0.31

[a] Refer to Chart 1 for the numbering scheme.

from the central carbon atom C_{cent}, as is particularly evident in Figure 3. At first glance, this observation might seem inconsistent with the experimental observation of a short (2.150 Å) Pt−C_{cent} bond distance in the crystal structure of **1**.[4c] We propose that this short bond distance is a result of the compromise between optimizing the C−C−C angle of the CH_2CCH^- fragment and the Pt−C_{term} bond lengths.

To investigate further the structure of **1**, density functional geometry optimization calculations were carried out on complex **1′** and another model complex, [(η^3-CH_2CCPh)$Pt(PH_3)_2$]$^+$ (**1″**). A comparison of calculated bond lengths and angles for the model complexes and the crystal structure of **1** is given in Table 1. The nonrelativistic optimization of **1′** gives good agreement with experiment for the C−C distances and C−C−C angle of the bound propargyl ligand. However, the Pt−ligand bond distances derived from the nonrelativistic calculation are consistently too long. The inclusion of scalar relativistic effects in the calculation considerably improves agreement with experiment, reproducing most of the Pt−ligand bond distances quite well. The largest deviations occur in the Pt−C_{term} distances, which are 0.066 Å too long and 0.084 Å too short for C1 and C3, respectively. Actually, the calculated distances for Pt−C1 and Pt−C3 are closer to the experimental distances for Pt−C3 and Pt−C1, respectively. This apparently worrisome result is not surprising, considering that the actual complex contains a phenyl group on C3, which has been replaced by a H atom in the calculation. The presence of a phenyl group on C3 should significantly affect the interaction of C3 with the metal center and consequently alter the interaction of Pt with C1. The inclusion of a phenyl group on C3 would be expected to improve agreement with experiment for these distances; hence, geometry optimization calculations on the model complex **1″** were performed. As indicated in Table 1, the inclusion of the phenyl group on C3 results in considerable improvement in both the calculated Pt−C1 and Pt−C3 distances. The error in the calculated Pt−C1 distance is now less than 0.01 Å, while the error in the Pt−C3 distance is 0.042 Å. In light of the above results it would also be interesting to compare the relativistic geometry optimization of **1′** to the structure of the [(η^3-CH_2CCH)$Pt(PPh_3)_2$]$^+$ complex recently prepared by Chen et al.[24] Unfortunately, no crystal structure for this complex has yet been reported.

Reactivity of 1. The reactions of nucleophiles with **1** have been extensively studied. With simple donor nucleophiles such as Br^-, PMe_3, and CO, nucleophilic addition occurs to the Pt center, resulting in the formation of η^1-propargyl and η^1-allenyl complexes. These reactions are consistent with a frontier-orbital-controlled nucleophilic attack that utilizes the Pt-localized 4a″ LUMO of **1′**.

The situation is more complicated when nucleophiles with a transferable proton (NuH) are used. These nucleophiles lead to apparent attack at the central carbon atom, which, after proton transfer, results in η^3-allyl complexes. This reactivity contrasts with that of nucleophiles with η^3-allyl complexes, which generally leads to addition to a terminal carbon of the allyl ligand.

To shed light on these reactivity differences, we have performed molecular orbital calculations on the model allyl complex [(η^3-CH_2CHCH_2)$Pt(PPh_3)_2$]$^+$ (**2′**) in a geometry modeled after the crystal structure of [(η^3-CH_2-$CHCH_2$)$Pt(PCy_3)_2$]$^+$.[15] In the model geometry, the terminal carbon atoms of the allyl ligand are coplanar with the Pt and P atoms, and the central carbon atom is tipped slightly away from the Pt atom (the dihedral angle between the C−C−C and the C_{term}−Pt−C_{term} planes is 109.4°). The MO diagram for **2′** is given in Figure 4, presented with fragment analysis analogous to that used in Figure 3 for complex **1′**.

At first sight, the electronic structure of allyl complex **2′** seems very similar to that of propargyl complex **1′**: The direct interaction of the Pt atom with C_{cent} is weak, and the LUMO of the complex is localized on the Pt $6p_z$ orbital. The central C atom carries a positive charge and

(24) Huang, T.-M.; Hsu, R.-H.; Yang, C.-S.; Chen. J.-T.; Lee, G.-H.; Wang, Y. *Organometallics* **1994**, *13*, 3657.

Table 2. Calculated Bond Distances (Å) and Angles (deg) for the Model Platinum Propargyl Complexes 1′ and 1″ Compared to Experimental Values for Complex 1[a]

	C1−C2	C2−C3	C1−C2−C3	Pt−C1	Pt−C2	Pt−C3	Pt−P1	Pt−P2	P1−Pt−P2
1 (exptl)[b]	1.39	1.23	152	2.186	2.150	2.273	2.262	2.297	100.2
1′	1.377	1.253	153.5	2.329	2.266	2.360	2.411	2.425	96.4
1′ (rel)[c]	1.387	1.263	149.7	2.252	2.161	2.189	2.254	2.265	95.7
1″ (rel)[c]	1.400	1.257	153.0	2.193	2.162	2.315	2.240	2.276	97.6

[a] Refer to Chart 1 for the numbering scheme of carbon atoms. [b] Reference 4c. [c] Calculation included scalar relativistic effects.

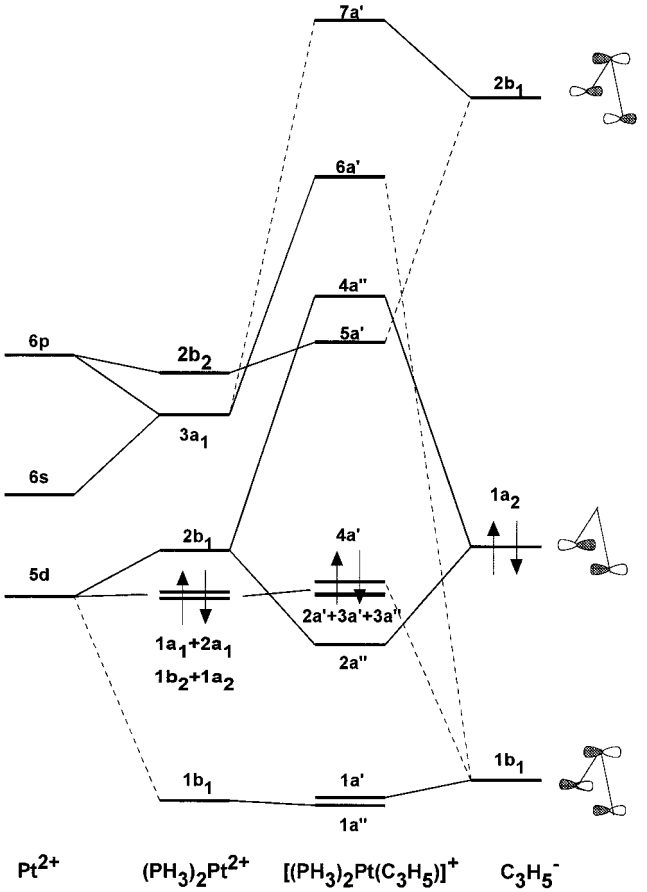

Figure 4. Molecular orbital diagram for the model allyl complex **2′**, $[(PH_3)_2Pt(\eta^3\text{-}CH_2CHCH_2)]^+$.

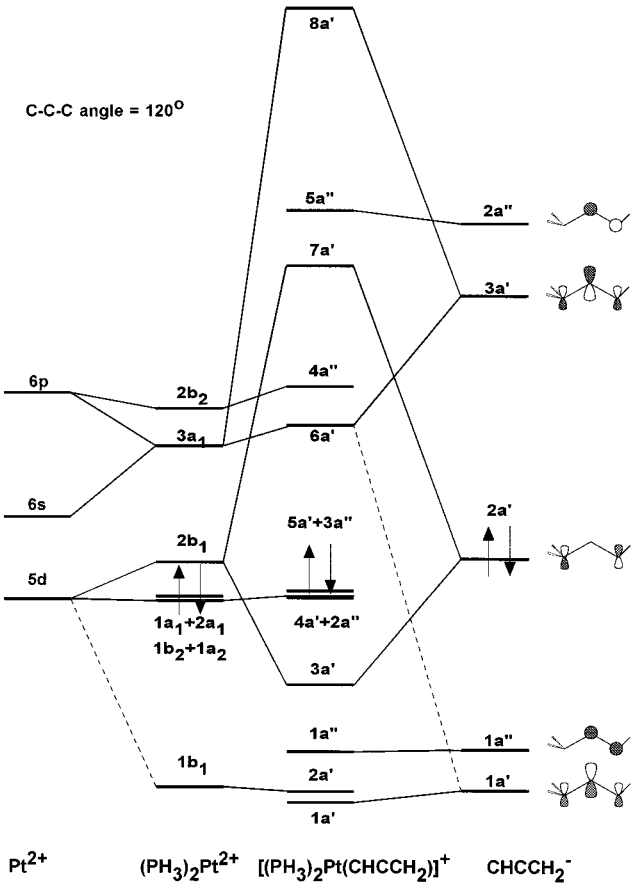

Figure 5. Molecular orbital diagram for the complex $[(PH_3)_2Pt(\eta^3\text{-}CHCCH_2)]^+$ (**1′**), with a C−C−C angle of 120°.

might therefore be the site of a charge-controlled nucleophilic attack. However, previous studies on these systems have indicated frontier-orbital control of the nucleophilic attack at C_{term} of the allyl ligand.[8] The 4a″ SLUMO (second lowest unoccupied MO) of **2′** has a node at C_{cent}. Further, because there is no low-lying virtual orbital that is localized on C_{cent}, the formation of a new bond at C_{cent} is not favored. Both the C_{term}-based 4a″ SLUMO and the Pt $6p_z$-based LUMO can act as good acceptor sites for frontier-orbital-controlled attack.

How does the above situation change in the propargyl complex **1′**? The 6a′ SLUMO of **1′** has very little C_{cent} character, like the 4a″ SLUMO of **2′**. Therefore, frontier-orbital control of nucleophilic attack of the propargyl ligand would seem to favor reaction at C_{term}. However, two factors serve to alter this analogy between the allyl and propargyl complexes. First, there is a greater degree of charge separation between C_{term} and C_{cent} in the propargyl ligand than in the allyl ligand. As shown in Table 2, the C_{cent} atom of the propargyl ligand is more positive and the C_{term} atoms are more negative than those in the allyl ligand. Thus, there is more likelihood that the reactivity of the propargyl ligand toward nucleophiles is charge-controlled. It is unclear whether the increased $C_{cent}-C_{term}$ charge separation would be sufficient to change the reactivity of the ligand so dramatically.

We propose that a second factor is involved in the difference in reactivity between **1′** and **2′**, namely the availability of a potential acceptor orbital in the propargyl ligand along the reaction pathway for nucleophilic attack. That is, after an initially charge-controlled approach by a nucleophile, the propargyl complex is capable of presenting the nucleophile with a low-energy acceptor orbital without drastically changing the geometry of the complex. To explore this effect further, we shall examine the changes in the electronic structure of **1′** as the C−C−C angle decreases, as it will upon formation of the allyl complex that is the ultimate product of the nucleophilic reaction.

Figure 5 presents the MO diagram for the propargyl complex **1′** in which the C−C−C angle of the propargyl ligand has been decreased from 152 to 120°. Upon this distortion, the 3a′ orbital of the CH_2CCH^- ligand drops below the 2a″ orbital, as described earlier. This change in orbital energetics, along with increased spatial

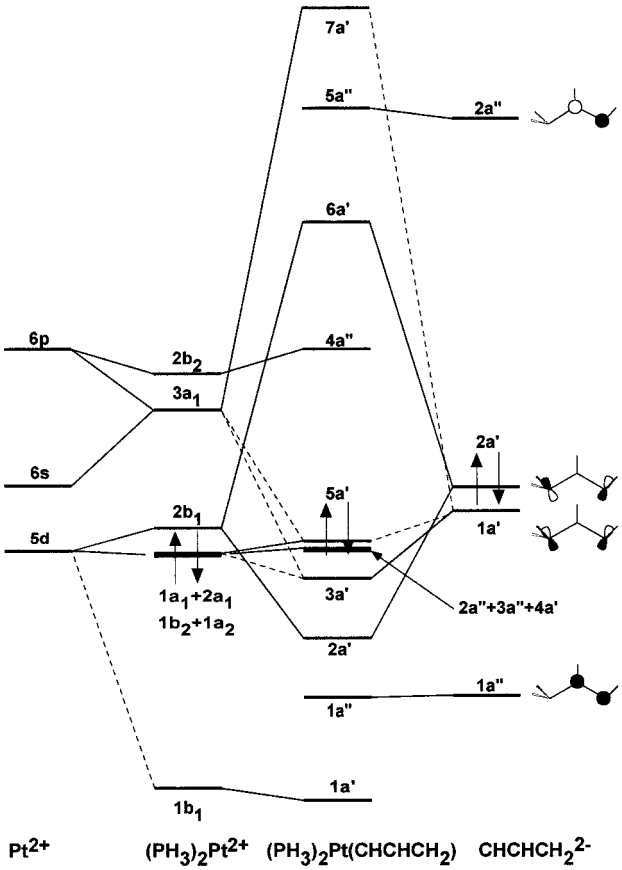

Figure 6. Molecular orbital diagram for the proposed metallacyclobutene intermediate complex $[(PH_3)_2Pt(\eta^2\text{-}CHCHCH_2)]$ (**3′**).

overlap, leads to a strong interaction between the 3a′ orbital of the CH_2CCH^- ligand and the $3a_1$ orbital of the $Pt(PH_3)_2^{2+}$ fragment. This interaction comprises the LUMO of **1′** in the distorted geometry, and the dominant contribution to this MO is from C_{cent} of the propargyl ligand. We therefore suggest that an initially charge-controlled interaction between the nucleophile and C_{cent} leads to distortion of the ligand to a metallacyclobutene-like intermediate with concomitant rehybridization of the C skeleton to an sp^2 central C atom. This pathway assists in the formation of the bond between C_{cent} and the nucleophile via the presentation of a low-lying acceptor orbital with significant C_{cent} character. There is no similar means of lowering the energy of the $2b_1$ orbital of the allyl ligand of **2′**. Thus, even if the initial approach of **2′** by the nucleophile is charge-controlled, there is no mechanism to provide a low-lying acceptor orbital for bond formation.

The Metallacyclobutene Intermediate. Casey and co-workers have isolated metallacyclobutene products in the reaction chemistry of η^3-propargyl complexes of Re.[25] We have proposed that a metallacyclobutene intermediate is likely in those reactions where nucleophiles add to the central carbon atom of platinum η^3-propargyl complexes.[26] A similar mechanism has also been suggested by Chen et al.[24] To investigate the possibility of such intermediates in this Pt chemistry, we have performed Fenske−Hall MO calculations on the model metallacyclobutene intermediate $(\eta^2\text{-}CH_2CHCH)Pt(PH_3)_2$ (**3′**). The MO diagram for this intermediate is presented in Figure 6. We find no significant interaction between the C−C π and π^* (1a″ and 2a″) MOs of the ligand and the $Pt(PH_3)_2^{2+}$ fragment. The ligand 2a′ orbital interacts strongly with the $2b_1$ orbital of $Pt(PH_3)_2^{2+}$, in a manner similar to that observed in the propargyl complex **1′**. Also like **1′**, the terminal carbon atoms of the $\eta^2\text{-}CH_2CHCH^{2-}$ ligand carry a significant negative charge (Table 2). We believe that the increased negative charge upon bending facilitates transfer of a proton from NuH to C3, resulting in the observed allyl complex. The absence of a transferable proton should lead to the isolation of the platinacyclobutene complex.

The recent synthesis of platinacyclobutenes through the reaction of $[(\eta^3\text{-}CH_2CCH)Pt(PPh_3)_2]^+$ with NEt_3, PPh_3, and C_5H_5N provides strong support for the notion of a metallacyclobutene intermediate.[27] Chen et al. have shown that protonation of the complex $[(\eta^2\text{-}CH_2C(PPh_3)CH)Pt(PPh_3)_2]^+$ leads to the formation of the η^3-allyl complex $[(\eta^3\text{-}CH_2C(PPh_3)CH_2)Pt(PPh_3)_2]^{2+}$, consistent with the suggestion that platinacyclobutene complexes may be intermediates in the reaction of **1** with nucleophiles of the type NuH.

Conclusions

The calculations presented here suggest that the primary interaction between platinum and the η^3-propargyl ligand in **1** occurs through the HOMO of the propargyl ligand, which is largely localized on the terminal carbon atoms of the ligand. The observed short platinum-to-central carbon atom distance arises as a result of maximizing overlap between the HOMO of the propargyl ligand and the platinum center and is not the result of a strong interaction between C_{cent} and Pt. Density functional calculations on the model complex **1′**, with the inclusion of scalar relativistic effects, accurately predict the structure of **1**. Increasing the complexity of the model complex by inclusion of a phenyl group on C3 results in further improvement in the predicted structure. We suggest that nucleophilic attack at the central carbon atom of the propargyl ligand occurs through an initially charge-controlled mechanism. However, the availability of a low-lying acceptor orbital along the reaction pathway assists the progress of the reaction. A metallacyclobutene intermediate is proposed, which lies along the suggested reaction pathway. A similar mechanism is not available in η^3-allyl complexes. We are currently carrying out density functional calculations in an attempt to further understand and map the reaction pathway.

OM9808209

(25) Casey, C. P.; Yi, C. S. *J. Am. Chem. Soc.* **1992**, *114*, 6597.

(26) Graham, J. P.; Bursten, B. E.; Wojcicki, A. *Abstracts of Papers*, 210th National Meeting of the American Chemical Society, Chicago, IL, August 1995; American Chemical Society: Washington, DC, 1995; INOR 77.

(27) Cheng, Y.-C.; Chen, Y.-K.; Huang, T.-M.; Yu, C.-I.; Lee, G.-H.; Wang, Y.; Chen, J.-T. *Organometallics* **1998**, *17*, 2953.